

## **Correlation Functions for Simple Fluids in a Finite System under Nonequilibrium Constraints**

**M. Malek Mansour<sup>1,2</sup>, John W. Turner,<sup>1</sup> and Alejandro L. Garcia<sup>1,2</sup>**

*Received April 17, 1987*

---

The Landau-Lifschitz fluctuating hydrodynamics formalism is applied to study the statistical properties of simple fluids in a finite system under nonequilibrium constraints. The boundary conditions are explicitly taken into account so that the results can be compared with particle simulations. Two scenarios are investigated: a fluid subjected to a constant shear and a fluid subjected to a constant temperature gradient. By considering a fluid with vanishing thermal expansivity, exact results are obtained for the static and dynamic correlation functions.

---

**KEY WORDS:** Fluctuating hydrodynamics; nonequilibrium systems; correlation functions; nonequilibrium fluctuations.

---

### **1. INTRODUCTION**

The statistical properties of physicochemical systems are known to change significantly when maintained out of equilibrium through appropriate external constraints, mainly because in a general nonequilibrium situation these constraints can keep the system in a state that would be highly improbable at equilibrium.<sup>(1)</sup> For this reason, a purely microscopic approach to the study of nonequilibrium systems proves to be far more difficult than at equilibrium. Model systems, based essentially on the theory of stochastic processes, have proved helpful and one of the simplest is a dilute mixture of molecules undergoing chemical reactions and diffusion. By modeling the chemical reactions through a birth and death process and the diffusion by a random walk it is possible to construct a stochastic game which, despite its simplicity, exhibits much of the complex behavior of a

---

<sup>1</sup> Université Libre de Bruxelles, Faculté des Sciences, B-1050 Bruxelles, Belgium.

<sup>2</sup> Center for Statistical Mechanics and Thermodynamics, University of Texas at Austin, Austin Texas 7812.

real reaction-diffusion system.<sup>(1-4)</sup> Using this theory, it is possible to understand the onset of spatial correlation from a near-equilibrium situation<sup>(5)</sup> up to the vicinity of a bifurcation point where the connection with equilibrium critical phenomena can be made.<sup>(6-10)</sup>

Stochastic approaches to the study of hydrodynamic systems also prove to be very helpful. In this respect, the most successful theory is undoubtedly the so-called "fluctuating hydrodynamics" of Landau and Lifschitz, in which spontaneous fluctuations of hydrodynamic variables are introduced into the transport equations by adding random components to the pressure and heat fluxes.<sup>(11)</sup> A few years ago it was realized that nonequilibrium modifications in the dynamical correlation function for hydrodynamic fluctuations were measurable in light scattering experiments.<sup>(12-15)</sup> The first such measurements were made on a liquid held at a fixed temperature gradient and they generated considerable interest.<sup>(16-19)</sup> Numerous theoretical approaches have been employed by various authors<sup>(20-26)</sup>; the Landau-Lifschitz theory, extended to nonequilibrium systems, is often used, mostly because of its relative simplicity as compared with more fundamental approaches.<sup>(14,26)</sup>

There remains, however, a paucity of experimental results, due to the numerous complications arising when performing small-angle scattering experiments. Precise line shapes are difficult to obtain. The performance of quantitative measurements is complicated by effects such as extraneous scattering, beam defocusing, etc. Another scenario that has been studied analytically is a fluid subject to a constant shear<sup>(15,27)</sup>; modifications to the scattered spectrum are as yet unobservable at rotation speeds that can be attained experimentally.<sup>(28)</sup>

Considering the technological limitations of laboratory experiments, another promising approach is by direct computer simulation. Molecular dynamics (MD) has led to a number of important advances in the theory of fluids, from the discovery of long-time tails<sup>(29,30)</sup> to the more recent observations of shear thinning<sup>(31,32)</sup> and shear freezing.<sup>(33)</sup> Traditionally, most MD work has been restricted to a microscopic regime best described by kinetic theory or generalized hydrodynamics. For example, the scattering function usually measured in MD is in the range of wavenumber typical of neutron scattering ( $\approx 1 \text{ \AA}^{-1}$ ). This is well outside the hydrodynamic range measured by light scattering ( $\approx 10^{-3} \text{ \AA}^{-1}$ ).<sup>(34)</sup>

Thanks to the newest generation of supercomputers, a number of macroscopic hydrodynamic phenomena have been recently reproduced (e.g., vortex formation and shedding past a flat plate<sup>(35)</sup> and past a cylinder<sup>(36)</sup>; convective rolls in the Rayleigh-Bénard system<sup>(37)</sup>). Such systems were previously considered beyond the capabilities of particle simulations (for a recent review see Ref. 38). Though the physical size of

the system remains relatively small ( $\approx 10^2$ – $10^3$  Å) and the applied constraints are often very large (e.g.,  $10^8$  K/cm<sup>(39)</sup>), the fluid is still very well described by the conventional hydrodynamic equations.

The measurement of the nonequilibrium modifications to the correlation functions directly from MD experiments has proved to be quite difficult and only qualitative results have been obtained.<sup>(40,41)</sup> In this respect, stochastic particle simulations based on the Boltzmann equation<sup>(42)</sup> have proved useful. By these simulations, various static correlations of density, velocity, and temperature have been measured<sup>(43)</sup> and shown to be in quantitative agreement with fluctuating hydrodynamic calculations.<sup>(44)</sup> This important new influx of data from computer experiments is stimulating renewed interest in analytical work.

The theoretical aspects of the problem, as relevant to computer experiments, present some important new features. First, the small system sizes and the strong gradients preclude the usual approximations developed for macroscopic systems (see Ref. 45 for a nice review). Second, the finite-size effects are of crucial importance and the boundary value problem must be considered with great care. Furthermore, as the system is typically closed, the conservation of total particle number plays an equally important role.

This paper is devoted specifically to obtaining exact results for the static and dynamic correlation functions in closed, finite systems. To do so, however, we must restrict ourselves to a simple fluid model where the thermal expansion coefficient vanishes (water at 4°C and normal fluid liquid helium near the  $\lambda$ -point satisfy this condition<sup>(46)</sup>). This model has already been used successfully by several authors<sup>(23,47,48)</sup> in the context of light scattering experiments. One may similarly work with more complex models, in which case the correlation functions for a finite system may be computed numerically.<sup>(49)</sup> Such numerical calculations have already been presented for the dilute gas equations and good agreement with computer experiment data was demonstrated.<sup>(44)</sup> Those results are qualitatively similar to the results presented here, a further indication of the utility of this model.

In the next section, we set up the fluctuating hydrodynamic equations in a finite geometry and discuss their general properties. Two nonequilibrium scenarios are subsequently studied in detail. In Section 3, we consider a simple fluid confined between two parallel planes moving with respect to each other at a given velocity. It is shown that the component of the velocity parallel to the moving planes obeys a closed non-Markovian equation which can be solved exactly; its static correlation function is found to be long-ranged. The dynamical correlation functions are also studied and interesting asymptotic behavior is found in the time correlation of fluctuations in density and in the perpendicular velocity. In Section 4, we

consider the case of a system subjected to a temperature gradient. Again, some of the resulting equal-time spatial correlation functions are found to be long-ranged; they may be compared qualitatively with recent Monte Carlo Boltzmann simulation data.<sup>(44)</sup> Explicit expressions for the density–density correlation function, which is associated with the light scattering spectrum, are obtained in Section 5. This scattering function is shown to display new maxima in a finite system. These new maxima are found to be asymmetric when the system is held under a fixed temperature difference in the same manner as the Brillouin peaks. In the conclusion we discuss the appropriateness of the model and point out the consequences of our results.

## 2. SIMPLE FLUID IN A FINITE SYSTEM

Consider a simple fluid confined between two parallel planes located at  $y = 0$  and  $y = L$ . These containing walls act as solid infinite reservoirs, so that by fixing their temperatures and tangential velocities, one can impose the desired temperature difference and strain on the system. The two boundaries perpendicular to these walls are taken as periodic boundaries; note that this construction is typical for molecular dynamics simulations.<sup>(39)</sup> As mentioned in the introduction, we restrict ourselves to a model with the following characteristics (see also Refs. 23 and 47):

1. The thermal expansion coefficient vanishes,

$$|\partial P_0 / \partial T_0|_{\rho_0} = 0 \quad (1)$$

2. The transport coefficients are constant (i.e., independent of density and temperature).
3. The state of the walls is statistically independent with respect to the state of the system.

By the first assumption, the momentum equation is decoupled from the energy equation. The last assumption implies a simple form for the boundary conditions, which is precisely the one realized in computer experiments with stochastic boundary conditions.<sup>(44,49)</sup> While these assumptions considerably simplify the analysis, the main physical aspects are preserved.

With this geometry and the above assumptions, the macroscopic hydrodynamic equations admit a steady-state solution of the form

$$T_0(\mathbf{r}) = T_0(y) \quad (2a)$$

$$P_0(\mathbf{r}) = P_0 = \text{const} \quad (2b)$$

$$\mathbf{u}_0(\mathbf{r}) = u_0(y) \mathbf{I}_x; \quad 0 \leq y \leq L \quad (2c)$$

where the subscript zero refers to macroscopic (i.e., nonfluctuating) quantities and  $\mathbf{I}_x$  is the unit vector in the  $x$  direction (strain direction). In the absence of external forces (e.g., gravity), this flow is stable<sup>(11)</sup> and the fluctuations are small.<sup>(50)</sup> In order to study the statistical properties of the system, we now linearize the fluctuating hydrodynamic equations around this macroscopic reference state to obtain

$$\partial_t \delta\rho(\mathbf{r}, t) = -\nabla \cdot (\rho_0 \delta\mathbf{u} + \mathbf{u}_0 \delta\rho) \quad (3)$$

$$\begin{aligned} \partial_t \delta u_i(\mathbf{r}, t) = & -(\mathbf{u}_0 \cdot \nabla) \delta u_i - (\delta\mathbf{u} \cdot \nabla) u_{0i} - \alpha \partial_i \delta\rho \\ & + \eta/\rho_0 \nabla^2 \delta u_i + (\frac{1}{3}\eta + \zeta)/\rho_0 \partial_i (\nabla \cdot \delta\mathbf{u}) - 1/\rho_0 \partial_j S_{ij}(\mathbf{r}, t) \end{aligned} \quad (4)$$

We employ the notation  $\partial_x \equiv \partial/\partial x$  with  $i, j, k, l \in \{x, y, z\}$ ;  $k_B$  is the Boltzmann constant,  $\eta$  and  $\zeta$  the shear and bulk viscosity coefficients, respectively, and  $\alpha$  is defined as

$$\alpha \equiv (1/\rho_0) |\partial P_0/\partial \rho_0|_{T_0} \quad (5)$$

The fluctuating part of the stress tensor  $S_{ij}$  is a white noise process in space and time; it is zero on average and its correlation function is given by<sup>(11)</sup>

$$\begin{aligned} \langle S_{ij}(\mathbf{r}, t) S_{kl}(\mathbf{r}', t') \rangle = & 2k_B T_0(y) [\eta (\delta_{ik} \delta_{jl} + \delta_{il} \delta_{jk}) \\ & + (\zeta - \frac{2}{3}\eta) \delta_{ij} \delta_{kl}] \delta(t - t') \delta(\mathbf{r} - \mathbf{r}') \end{aligned} \quad (6)$$

Since the macroscopic pressure is a constant, so are  $\alpha$  and  $\rho_0$ . In spite of these simplifying assumptions, finding the explicit solution of these equations in their general form proves to be a rather difficult task, mainly because of the boundary value problem. Nevertheless, the problem can be solved exactly if we restrict ourselves to reduced variables defined by

$$\delta h(y) = \frac{1}{S} \int_0^{L_x} dx \int_0^{L_z} dz \delta h(x, y, z) \quad (7)$$

where  $h$  is any hydrodynamic variable and  $S \equiv L_x L_z$  is the surface area of the walls. Note that these reduced variables are in fact the zero-wavevector values of the ‘‘parallel’’ Fourier components of the hydrodynamic variables. From now on we shall only treat reduced variables. With periodic boundary conditions in the  $x$  and  $z$  directions, the fluctuating hydrodynamic equations in reduced quantities are

$$\partial_t \delta\rho = -\rho_0 \partial_y \delta v \quad (8)$$

$$\partial_t \delta u = -\varphi \delta v + \eta/\rho_0 \partial_y^2 \delta u + 1/\rho_0 \partial_y f_x(y, t) \quad (9)$$

$$\partial_t \delta v = -\alpha \partial_y \delta\rho + 1/\rho_0 (\frac{4}{3}\eta + \zeta) \partial_y^2 \delta v + 1/\rho_0 \partial_y f_y(y, t) \quad (10)$$

$$\partial_t \delta w = \eta/\rho_0 \partial_y^2 \delta w + 1/\rho_0 \partial_y f_z(y, t) \quad (11)$$

with

$$\begin{aligned} \langle f_x(y, t) f_x(y', t') \rangle &= \langle f_z(y, t) f_z(y', t') \rangle \\ &= 2k_B T_0(y) \eta / S \delta(y - y') \delta(t - t') \end{aligned} \quad (12a)$$

$$\langle f_y(y, t) f_y(y', t') \rangle = 2k_B T_0(y) (\frac{4}{3}\eta + \zeta) / S \delta(y - y') \delta(t - t') \quad (12b)$$

$$\langle f_i(y, t) f_j(y', t') \rangle = 0 \quad \text{for all } i \neq j \quad (12c)$$

where  $\delta u$ ,  $\delta v$ , and  $\delta w$  are the  $x$ ,  $y$ , and  $z$  velocity fluctuations, respectively, and  $\varphi(y) \equiv \partial u_0 / \partial y$  is the shear.

It is useful to point out some interesting properties of the reduced equations. First, the  $z$  component of the reduced velocity fluctuations  $\delta w$  is decoupled from the other variables and it is not influenced by the constraint. Second, the equation for the  $y$  component  $\delta v$  is coupled only to the continuity equation. In the next sections we shall see that these properties greatly simplify the analysis while preserving most of the typical nonequilibrium effects. In the conclusion, we further argue the validity of using these reduced variables. Moreover, in most of the nonequilibrium computer simulations, a space average over the parallel directions is taken (mainly to increase the accuracy of the statistics) so that the effective variables measured are precisely the reduced variables considered here.

There remains the problem of specifying the boundary conditions for Eqs. (8)–(11). The boundary conditions for  $\delta v$  follow from the conservation of total particle number,

$$\int_0^L dy \delta \rho(y, t) = 0 \quad (13)$$

The continuity equation yields

$$\rho_0 \delta v(y) |_{\text{boundaries}} = 0 \quad (14)$$

i.e., the boundary acts as a perfectly rigid wall. The boundary conditions for  $\delta u$  and  $\delta w$  are as those of a no-slip wall:

$$\delta u(y=0) = \delta u(y=L) = \delta w(y=0) = \delta w(y=L) = 0 \quad (15)$$

These relations are a consequence of our third assumption that the state of the walls is statistically independent with respect to the state of the system. In fact, one can always consider an enlarged description in which the state of the walls is included as well. The evolution is then governed by a global probability density, which factorizes into system variables and wall variables; an average over the wall variables leaves one with a stochastic

process for the system variables only. A straightforward change of variables then leads to the relations (14) and (15). Note that this in no way contradicts the fact that the wall variables can also be considered as fluctuating variables, as is usually done in computer experiments (stochastic boundary conditions<sup>(39,51)</sup>).

No boundary condition for  $\delta\rho$  is required, as its evolution is entirely specified by the initial conditions for  $\delta\rho$  and  $\delta\mathbf{u}$  plus the boundary conditions for  $\delta\mathbf{u}$ . From a physical point of view, this reflects the fact that the state of the wall can only constrain the temperature and velocity of the fluid at the wall, whereas the behavior of the density close to the wall is entirely determined by the internal dynamics of the system. The mathematical aspects of the specification of the boundary conditions are discussed in the Appendix.

Given this boundary condition for  $\delta\mathbf{u}$  and the continuity equation, it is easy to show that the reduced fluctuations can be expanded in the following sine and cosine series:

$$\delta\rho(y, t) = \sum_{k=0}^{\infty} \delta\rho_k(t) \cos \frac{k\pi y}{L} \tag{16a}$$

$$\begin{pmatrix} \delta u(y, t) \\ \delta v(y, t) \\ \delta w(y, t) \end{pmatrix} = \sum_{k=0}^{\infty} \begin{pmatrix} \delta u_k(t) \\ \delta v_k(t) \\ \delta w_k(t) \end{pmatrix} \sin \frac{k\pi y}{L} \tag{16b}$$

with the well-known inverse formula

$$\delta\rho_k(t) = \frac{2}{L} \int_0^L dy \delta\rho(y, t) \cos \frac{k\pi y}{L}; \quad \delta\rho_0(t) = 0 \tag{16c}$$

$$\begin{pmatrix} \delta u_k(t) \\ \delta v_k(t) \\ \delta w_k(t) \end{pmatrix} = \frac{2}{L} \int_0^L dy \begin{pmatrix} \delta u(y, t) \\ \delta v(y, t) \\ \delta w(y, t) \end{pmatrix} \sin \frac{k\pi y}{L} \tag{16d}$$

In this paper, we restrict ourselves to the study of the statistical properties of a system in the stationary regime (i.e., we are not considering the transient regimes where one studies the evolution from a given initial condition). In this regime, a common approach is to use the Fourier transform in time,

$$\delta h(t) = \int_{-\infty}^{\infty} d\omega \delta h(\omega) e^{-i\omega t} \tag{17a}$$

$$\delta h(\omega) = \frac{1}{2\pi} \int_{-\infty}^{\infty} dt \delta h(t) e^{i\omega t} \tag{17b}$$

where  $h$  is any hydrodynamic variable.

Equations (8)–(11) may now easily be solved by using the above transforms, and the various correlation functions could be constructed in  $(k, \omega)$  space. This, however, is not their most useful representation. For example, in computer experiments, density fluctuations are commonly probed by measuring the Van Hove total correlation function,<sup>(52)</sup>

$$G_q(t) = \frac{1}{N} \left\langle \sum_{a=1}^N \exp \frac{i2\pi q \mathbf{I}_y \cdot \mathbf{r}_a(t)}{L} \sum_{b=1}^N \exp \frac{-i2\pi q \mathbf{I}_y \cdot \mathbf{r}_b(t=0)}{L} \right\rangle \quad (18)$$

where  $\mathbf{r}_a$  and  $\mathbf{r}_b$  are the positions of particles  $a$  and  $b$ , respectively,  $\mathbf{I}_y$  is the unit vector in the  $y$  direction, and  $N$  is the total number of particles in the system. At hydrodynamic scales, this function is equivalent to the scattering function, defined as (see, e.g., Ref. 52)

$$S_q(\omega) = \frac{V}{\rho_0 m L^2} \int_0^L dy \int_0^L dy' \exp \frac{i2\pi q(y-y')}{L} \\ \times \int_{-\infty}^{\infty} d\omega' \langle \delta\rho(y, \omega) \delta\rho(y', \omega') \rangle \quad (19)$$

where  $m$  is the particle mass. This scattering function can also be obtained in light scattering experiments from the measured spectrum.<sup>(34,53)</sup> In the limit of large equilibrium systems,  $S_q(\omega)$  may be computed directly from  $\langle \delta\rho(k, \omega) \delta\rho(k', \omega') \rangle$  by the replacement  $k \rightarrow 2q$ ,  $k' \rightarrow 2q$ . In finite systems, there is no similar simple step; we must first obtain the density fluctuations in real space and then compute  $S_q(\omega)$  according to Eq. (19) (cf. Section 5).

Note finally that another way to proceed is to construct first the governing equations for the correlation functions and solve them directly. This method has been already discussed in Refs. 44 and 49. Its main advantage over the more traditional method discussed above comes from the fact that it leads directly to numerical solutions when the problem is too complicated to be handled analytically.

At this point it is instructive to consider the effects of shear and heat flux separately, as the resulting phenomena are very different. Also, most experiments (computer and laboratory) are conducted in one of the two regimes:  $\{u_0 \neq 0, \partial T_0 / \partial y = 0\}$  or  $\{u_0 = 0, \partial T_0 / \partial y \neq 0\}$ .

### 3. SIMPLE FLUID UNDER A CONSTANT SHEAR

In this section we consider the case of a simple fluid under a constant strain. Due to viscous heating, the fluid develops a parabolic temperature profile whose amplitude is proportional to the square of the velocity gradient. If the imposed strain is not too large, the temperature variation is

very small and, for simplicity, we shall take the temperature as constant. Our evolution equations (8)–(11) do not simplify, but the noise correlations, Eqs. (12), are no longer space-dependent, and, as a consequence, the equations for  $\delta\rho$ ,  $\delta v$ , and  $\delta w$  are unaffected by the constraint. By the use of the transforms defined in the previous section, we immediately obtain the correlation functions for these variables:

$$\langle \delta\rho_k(\omega) \delta\rho_{k'}(\omega') \rangle = \frac{4k_B\rho_0 T_0 \Gamma}{\pi V} \frac{k^4 \pi^4 / L^4 \delta(\omega + \omega') \delta_{kk'}}{[\omega^2 - (ck\pi/L)^2]^2 + 4\omega^2 \Gamma^2 k^4 / L^4} \quad (20)$$

$$\langle \delta v_k(\omega) \delta v_{k'}(\omega') \rangle = \frac{4k_B T_0 \Gamma}{\rho_0 \pi V} \frac{\omega^2 k^2 \pi^2 / L^2 \delta(\omega + \omega') \delta_{kk'}}{[\omega^2 - (ck\pi/L)^2]^2 + 4\omega^2 \Gamma^2 k^4 \pi^4 / L^4} \quad (21)$$

$$\langle \delta w_k(\omega) \delta w_{k'}(\omega') \rangle = \frac{2k_B T_0 \eta}{\pi V \rho_0^2} \frac{\delta(\omega + \omega') \delta_{kk'} k^2 \pi^2 / L^2}{(\eta/\rho_0)^2 k^4 \pi^4 / L^4 + \omega^2} \quad (22)$$

$$\langle \delta\rho_k(\omega) \delta v_{k'}(\omega') \rangle = -i\rho_0 (k\pi/\omega L) \langle \delta v_k(\omega) \delta v_{k'}(\omega') \rangle \quad (23)$$

$$\langle \delta\rho_k(\omega) \delta w_{k'}(\omega') \rangle = \langle \delta v_k(\omega) \delta w_{k'}(\omega') \rangle = 0 \quad (24)$$

where  $V$  is the volume of the system ( $V = SL$ ),  $\Gamma$  is the sound damping coefficient, and  $c$  is the sound speed:

$$\Gamma = (\frac{4}{3}\eta + \zeta)/2\rho_0 \quad (25)$$

$$c = (\alpha\rho_0)^{1/2} \quad (26)$$

Let us first focus on the static correlation functions. For the density  $\delta\rho$  and velocities  $\delta v$  and  $\delta w$ , one easily finds

$$\langle \delta v(y) \delta v(y') \rangle = \langle \delta w(y) \delta w(y') \rangle = (k_B T_0 / \rho_0 S) \delta(y - y') \quad (27)$$

$$\langle \delta v(y) \delta w(y') \rangle = 0 \quad (28)$$

$$\langle \delta\rho(y) \delta\rho(y') \rangle = (k_B T_0 / \alpha S) [\delta(y - y') - 1/L] \quad (29)$$

which are clearly the results we expect from equilibrium statistical mechanics.<sup>(50)</sup> The term  $-1/L$  in Eq. (29) ensures the conservation of the total mass. Because of this term, the static density autocorrelation function is strictly negative and its integral compensates for the local equilibrium (delta function) contribution.

Now consider the equation for the  $x$  component of the reduced velocity, which depends on the macroscopic velocity gradient  $\varphi \equiv \partial u_0 / \partial y$  and may be written as

$$\partial_t \delta u = \eta / \rho_0 \partial_y^2 \delta u + F(y, t) \quad (30)$$

where  $F(y, t)$  is an effective noise term:

$$\langle F(y, t) \rangle = 0 \tag{31}$$

$$\begin{aligned} \langle F(y, t) F(y', t') \rangle &= 2k_B T_0 \eta / (\rho_0^2 S) \partial_y \partial_{y'} \delta(y - y') \delta(t - t') \\ &+ \varphi(y) \varphi(y') \langle \delta v(y, t) \delta v(y', t') \rangle \end{aligned} \tag{32}$$

This is a *non-Markovian* equation for  $\delta u(y, t)$ , since  $\langle \delta v(y, t) \delta v(y', t') \rangle$  is *not* delta-correlated in time. Note that Eq. (30) can be used as a starting point for a more phenomenological theory; for this reason we shall first derive its formal solution without reference to the explicit form of  $\varphi(y)$  or  $\langle \delta v \delta v' \rangle$ . Again, using the transforms defined in Section 2, one finds

$$\delta u_k(\omega) = \frac{-\beta_k(\omega)}{k^2 \pi^2 / (\rho_0 L^2) - i\omega} - \frac{k\pi / (\rho_0 L) \psi_k(\omega)}{k^2 \pi^2 / (\rho_0 L^2) - i\omega} \tag{33}$$

where  $\psi_k(\omega)$  is the Fourier transform of  $f_x$ ,

$$\langle \psi_k(\omega) \psi_{k'}(\omega') \rangle = 2k_B T_0 \eta / (\pi V) \delta_{kk'} \delta(\omega + \omega') \tag{34}$$

and

$$\beta_k(\omega) \equiv 2/L \int_0^L dy \sin(k\pi y/L) \varphi(y) \delta v(y, \omega) \tag{35}$$

Due to the absence of correlation between Langevin source terms, we have

$$\langle \beta_k(\omega) \psi_{k'}(\omega') \rangle = \langle \delta v_k(\omega) \psi_{k'}(\omega') \rangle = 0 \tag{36}$$

$$\langle \beta_k(\omega) \beta_{k'}(\omega') \rangle = \sum_{n=0}^{\infty} \sum_{n'=0}^{\infty} \varphi_{k,n} \varphi_{k',n'} \langle \delta v_n(\omega) \delta v_{n'}(\omega') \rangle \tag{37}$$

$$\varphi_{k,n} = 2/L \int_0^L dy \sin(k\pi y/L) \sin(n\pi y/L) \varphi(y) \tag{38}$$

which completes the solution of Eq. (30).

In our case,  $\varphi$  does not depend on position and the relation (38) becomes simply

$$\varphi_{k,n} = \varphi \delta_{kn} \tag{39}$$

Hence

$$\beta_k(\omega) = \varphi \delta v_k(\omega) \tag{40}$$

This finally gives

$$\begin{aligned} \langle \delta u_k(\omega) \delta u_k(\omega') \rangle &= \frac{1}{(\eta/\rho_0)^2 k^4 \pi^4 / L^4 + \omega^2} \left( \varphi^2 \langle \delta v_k(\omega) \delta v_k(\omega') \rangle \right. \\ &\quad \left. + \frac{2k_B T_0 \eta}{\pi V \rho_0^2} \delta_{k,k'} \delta(\omega + \omega') \frac{k^2 \pi^2}{L^2} \right) \end{aligned} \quad (41)$$

The second term is just the local equilibrium contribution, while the first term expresses the nonequilibrium contribution. Using the explicit form of  $\langle \delta v_k(\omega) \delta v_k(\omega') \rangle$  [Eq. (21)], one finds after some algebra

$$\begin{aligned} \langle \delta u(y) \delta u(y') \rangle &= \frac{k_B T_0}{\rho_0 S} \delta(y - y') \\ &= \frac{\varphi^2 k_B T_0}{c^2 \rho_0 S} \\ &\quad \times \left\{ y' \left( 1 - \frac{y}{L} \right) - \frac{\lambda \cosh[(y - y' - L)/\lambda] - \cosh[(y + y' - L)/\lambda]}{2 \sinh(L/\lambda)} \right\} \end{aligned} \quad (42)$$

with  $y \geq y'$  (for  $y < y'$ , exchange  $y$  and  $y'$ ) and

$$\lambda = [\eta(\zeta + \frac{7}{3}\eta)]^{1/2} / (c\rho_0) \quad (43)$$

Our  $\lambda$ , which has the units of length, can be associated with an acoustic absorption scale. The dimensionless parameter  $L/\lambda$  appears as the ratio of the inertial to the viscous effects. This parameter resembles the Reynolds number, except that the characteristic flow speed is taken to be the sound speed.

If  $\lambda \ll L$ , the second term in the brackets in Eq. (42) is negligible and the nonequilibrium part of  $\langle \delta u \delta u' \rangle$  reduces to a piecewise linear function whose amplitude is proportional to the square of the amplitude of the constraint (see Fig. 1). This is reminiscent of the results of Ref. 5 for the temperature autocorrelation function in a high-Prandtl-number liquid (see also Refs. 43, 44, 49, and 54) and of the results of Ref. 55 for the density autocorrelation function in a lattice gas. For  $\lambda \gg L$ , the entire nonequilibrium effect vanishes. Recent stochastic particle simulation results for a dilute gas under shear demonstrate nice qualitative agreement with Eq. (42).<sup>(56)</sup>

Let us now turn our attention to the behavior of the dynamical

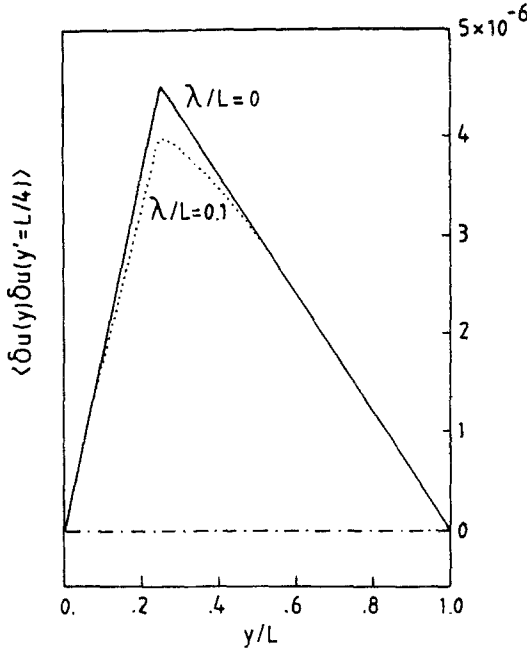


Fig. 1. The nonequilibrium component of  $\langle \delta u(y) \delta u(y') \rangle_{st}$  for  $y' = L/4$  versus  $y/L$  [see Eq. (42)]. The parameters are taken from the simulation described in Ref. 56 [ $T_0 = 1$ ,  $\varphi = 1/25$ ,  $L_x = L_z = 1$ ,  $\eta_0 = 5/16\rho_0 (\pi T_0)^{1/2}$ ,  $\zeta = 0$ ,  $c = (5/3k_B/mT_0)^{1/2}$ ,  $k_B/m = 1/2$ ,  $m = 1$ ,  $\rho_0 = 400$ ], with varying values of system length. The system is under a constant shear; the temperature gradient is assumed to be negligible.

correlation functions. For the  $z$  component  $\delta w$  of the reduced velocity one easily finds

$$\begin{aligned} \langle \delta w(y, t) \delta w(y', 0) \rangle &= 2(k_B T_0 / \rho_0 V) \sum_{k=1}^{\infty} \sin(k\pi y/L) \sin(k\pi y'/L) \\ &\times \exp(-\eta k^2 \pi^2 t / \rho_0 L^2) \end{aligned} \quad (44)$$

which shows that each spatial Fourier mode decays exponentially. To study this expression, we shall assume that the system size  $L$  is large enough so that the series can be replaced by an integral. In this limit,

$$\begin{aligned} \langle \delta w(y, t) \delta w(y', 0) \rangle &= (k_B T_0 / \rho_0 S) (\rho_0 / 4\pi\eta t)^{1/2} \\ &\times \{ \exp[-\rho_0(y - y')^2 / 4\eta t] - \exp[-\rho_0(y + y')^2 / 4\eta t] \} \end{aligned} \quad (45)$$

which in the long-time limit behaves as

$$\lim_{t \rightarrow \infty} \langle \delta w(y, t) \delta w(y', 0) \rangle \propto O(t^{-3/2}) \tag{46}$$

which is a well-known result.<sup>(52)</sup>

In contrast, the density and perpendicular velocity correlation functions exhibit a more interesting long-time behavior (see Section 5 for a full discussion of the scattering function). Consider,

$$\begin{aligned} &\langle \delta v(y, t) \delta v(y', 0) \rangle \\ &= \sum_{k=0}^{\infty} \sum_{k'=0}^{\infty} \sin(k\pi y/L) \sin(k'\pi y'/L) \\ &\quad \times \int_{-\infty}^{\infty} d\omega \int_{-\infty}^{\infty} d\omega' e^{-i\omega t} \langle \delta v(k, \omega) \delta v(k', \omega') \rangle \end{aligned} \tag{47}$$

To evaluate this function, we first set  $\omega = iz$ ; it follows from (21) that for large  $L$  we can write

$$\begin{aligned} &\langle \delta v(y, t) \delta v(y', 0) \rangle \\ &= \frac{k_B T_0 \rho_0}{2\pi^2 S} \int_0^{\infty} dq [\cos q\pi(y - y') - \cos q\pi(y + y')] I_q \end{aligned} \tag{48}$$

with

$$I_q = i \int_{-i\infty}^{i\infty} dz z e^{zt} \left( \frac{1}{z^2 + 2z\Gamma q^2 + c^2 q^2} - \frac{1}{z^2 - 2z\Gamma q^2 + c^2 q^2} \right) \tag{49}$$

As  $t > 0$ , we shall close the contour to the left, so that the second term in (49) can be dropped, as its poles lie in the half-plane  $\text{Re } z > 0$ . We are left with an expression of the form

$$J(r) = \int_{-\infty}^{\infty} dq \cos r q \int_{-i\infty}^{i\infty} dz z e^{zt} (z^2 + 2z\Gamma q^2 + c^2 q^2)^{-1} \tag{50}$$

where  $r = |y \pm y'|$ . To evaluate  $J(r)$ , we next exchange the order of integration to obtain

$$J(r) = \pi/2 \int_{-i\infty}^{i\infty} dz (2z\Gamma + c^2)^{-1/2} \exp[zt + rz(2z\Gamma + c^2)^{-1/2}] \tag{51}$$

The contour can now be shifted to the left up to the branch point at  $z = -c^2/2\Gamma$ . Setting  $z = s^2 - c^2/2\Gamma$ , one finds

$$J(r) = \frac{\pi \exp(-c^2 t/2\Gamma)}{(2\Gamma)^{1/2}} \int_C ds \exp \left[ ts^2 + \frac{r(s - c^2/2\Gamma s)}{(2\Gamma)^{1/2}} \right] \tag{52}$$

where  $C$  moves into the origin from  $(+\infty)e^{-i\pi/4}$  and goes out to  $(+\infty)e^{+i\pi/4}$ . For large  $t$ , the dominant contributions to this integral come from two saddle points lying in the vicinity of  $s=0$  at  $t^{-1/3}(2\Gamma)^{-1/2}(rc^2/2)^{1/3}e^{\pm i\pi/3}$ , and thus we have

$$J(r) \propto t^{-1/2} \exp(-c^2t/2\Gamma - at^{1/3}r^{2/3}c^{4/3}/\Gamma) \quad (53)$$

where  $a$  is a numerical constant whose precise value is not important in this context. Finally, for  $y$  and  $y'$  of the order of  $L$ , the contribution to (53) comes mainly from  $r = |y - y'|$ , which leads to the result

$$\begin{aligned} & \lim_{t \rightarrow \infty} \langle \delta v(y, t) \delta v(y', 0) \rangle \\ & \propto t^{-1/2} \exp[-c^2t/2\Gamma - at^{1/3}|y - y'|^{2/3}c^{4/3}/\Gamma] \end{aligned} \quad (54)$$

From our original equations (8) and (10), it is clear that the reduced density and perpendicular velocity fluctuations cannot be affected by the velocity gradient. The peculiar asymptotic behavior we find for  $\langle \delta v(y, t) \delta v(y', t') \rangle$  is not a nonequilibrium effect; it is present at equilibrium.

We will not explicitly present the dynamic correlation function for the  $x$  component of the reduced velocity, but only remark that its asymptotic behavior is the same as that of  $\delta w$  [Eq. (46)]. This is reasonable, since in the limit of vanishing velocity gradient, they obey the same equation [compare (22) and (41) with  $\varphi = 0$ ] and in the limit  $t \rightarrow \infty$ , the coupling with  $\langle \delta v \delta v' \rangle$  is of negligible contribution.

We see that for finite systems, such as those that can be realized in computer simulations, the decay of each mode of the correlation function remains essentially exponential. According to these asymptotic results, however, one should observe distinct time scales between the  $y$  component of the fluctuating velocity  $\delta v$  (and the fluctuating density  $\delta\rho$ ) on the one hand, and the  $x$  and  $z$  components of the fluctuating velocity  $\delta u$  and  $\delta w$  on the other (see Fig. 2).

Before closing this section, we should like to clarify an important point about the dynamic (reduced) density correlations in systems under shear. As we remark, the velocity gradient produces no modification to  $\langle \delta\rho(y, t) \delta\rho(y', t') \rangle$ , yet this is a direct consequence of our setting the parallel Fourier component  $k_{\parallel}$  to zero. For nonzero  $k_{\parallel}$ , the continuity equation is coupled to the  $\delta u$  equation and, as a consequence, the density autocorrelation function does depend on the shear. The scattering function [Eq. (19)] remains symmetric, but the heights of the Brillouin lines are modified linearly with respect to the imposed shear. This property was predicted by Machta *et al.*,<sup>(27,28)</sup> but remains unobserved in laboratory

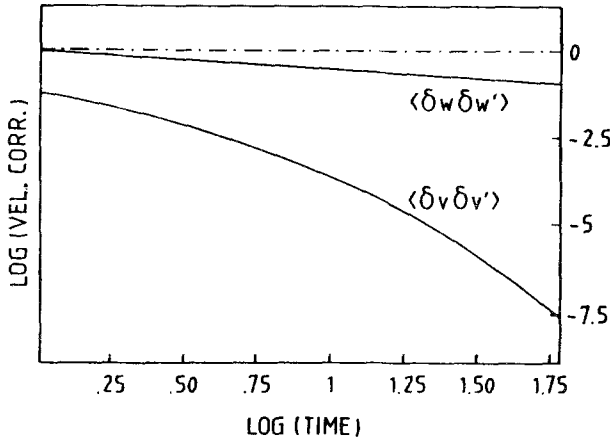


Fig. 2. The asymptotic forms ( $t \rightarrow \infty$ ) of  $\langle \delta w(y, t) \delta w(y', 0) \rangle$  and  $\langle \delta v(y, t) \delta v(y', 0) \rangle$  for  $y = y' = L/2$  versus time. The parameters are taken from the simulation described in Ref. 56 ( $L = 10$ ; see caption to Fig. 1 for the other parameters).

experiments because of technical difficulties. The computation of the finite-size effect for the  $k_{\parallel} \neq 0$  case is quite tedious and will be reported elsewhere. A full discussion of the scattering function for reduced density fluctuations ( $k_{\parallel} = 0$ ) is presented in Section 5.

#### 4. FINITE SYSTEM UNDER A CONSTANT HEAT FLUX

In this section, we consider the case of a fixed temperature gradient  $\gamma$ , but with no shear ( $\varphi = 0$ ). Our original equations (8)–(11) simplify in that the equation for  $\delta u$  is now decoupled from the rest, but the coefficients in the noise correlations [Eqs. (12)] are space-dependent, since the macroscopic temperature is no longer uniform and is given by

$$T_0(y) = T(y = 0) + \gamma y \tag{55}$$

The nonequilibrium effects in this case come therefore from the inhomogeneous distribution of the Langevin sources.

It is easy to check that the parallel components of the velocity fluctuations are not affected by the constraint, so that we shall concentrate only on the density and perpendicular velocity fluctuations  $\delta \rho$  and  $\delta v$ . Using the transforms defined in Section 2, one finds

$$\langle \delta \rho_k(\omega) \delta \rho_{k'}(\omega') \rangle = \frac{4k_B \Gamma \rho_0 \delta(\omega + \omega')}{\pi V (c^4 + 4\omega^2 \Gamma^2)} T_{k,k'} \frac{k^2}{k^2 - z^2} \frac{k'^2}{k'^2 - z'^2} \tag{56}$$

$$\langle \delta v_k(\omega) \delta v_{k'}(\omega') \rangle = \frac{\omega^2}{\rho_0^2(k\pi/L)(k'\pi/L)} \langle \delta \rho_k(\omega) \delta \rho_{k'}(\omega') \rangle \quad (57)$$

$$\langle \delta \rho_k(\omega) \delta v_{k'}(\omega') \rangle = \frac{i\omega'}{\rho_0(k'\pi/L)} \langle \delta \rho_k(\omega) \delta \rho_{k'}(\omega') \rangle \quad (58)$$

where the function  $T_{k,k'}$  is defined as

$$T_{k,k'} = \frac{1}{2L} \int_0^L dy \cos \frac{k\pi y}{L} \cos \frac{k'\pi y}{L} T_0(y) \quad (59)$$

and we have set

$$z^2 = \frac{\omega^2 L^2 (c^2 + 2i\omega\Gamma)}{\pi^2 (c^4 + 4\omega^2 \Gamma^2)} \quad (60)$$

As in the previous section, we shall first study the static correlation functions. Integrating the relations (56)–(58) over  $\omega$  and  $\omega'$  and separating the local equilibrium contributions, one finds

$$\begin{aligned} \langle \delta \rho(y) \delta \rho(y') \rangle_{\text{st}} &= \frac{k_B T_0(y)}{\alpha S} \delta(y - y') \\ &= -\frac{k_B}{\alpha V} [T_0(y) + T_0(y') - T_a] \\ &\quad + \frac{8k_B \rho_0 \gamma}{c^2 \pi^2 S} \sum_{k+k'=\text{odd}} \sum \cos \left( \frac{k\pi y}{L} \right) \cos \left( \frac{k'\pi y'}{L} \right) \frac{k^2 + k'^2}{\Delta_{kk'}} \end{aligned} \quad (61)$$

$$\begin{aligned} \langle \delta v(y) \delta v(y') \rangle_{\text{st}} &= \frac{k_B T_0(y)}{\rho_0 S} \delta(y - y') \\ &= \frac{16k_B \gamma}{\rho_0 \pi^2 S} \sum_{k+k'=\text{odd}} \sum \sin \left( \frac{k\pi y}{L} \right) \sin \left( \frac{k'\pi y'}{L} \right) \frac{kk'}{\Delta_{kk'}} \end{aligned} \quad (62)$$

$$\begin{aligned} \langle \delta \rho(y) \delta v(y') \rangle_{\text{st}} \\ &= \frac{32k_B \gamma \varepsilon}{c\pi S} \sum_{k+k'=\text{odd}} \sum \cos \left( \frac{k\pi y}{L} \right) \sin \left( \frac{k'\pi y'}{L} \right) \frac{(k^2 + k'^2) k^2 k'}{(k^2 - k'^2) \Delta_{kk'}} \end{aligned} \quad (63)$$

where  $T_a \equiv 1/L \int_0^L dy T_0(y)$  is the space-averaged temperature,

$$\Delta_{kk'} = (k^2 - k'^2)^2 + 8\pi^2 \varepsilon^2 k^2 k'^2 (k^2 + k'^2) \quad (64)$$

and  $\varepsilon$  is a dimensionless number defined as

$$\varepsilon = \Gamma/cL \quad (65)$$

The double sums in (61)–(63) are quite difficult to evaluate explicitly, except asymptotically in the limit  $\varepsilon \rightarrow 0$ . Yet for small values of  $L$  [ $\varepsilon \sim O(1)$ ], the double sums for  $\langle \delta\rho \delta\rho' \rangle$  and  $\langle \delta v \delta v' \rangle$  are easily computed numerically, since they converge as  $O(k^{-4})$  (see Fig. 3). This is not the case for  $\langle \delta\rho \delta v' \rangle$ , which behaves as  $O(k^{-2})$ , indicating the possible presence of a discontinuity in the derivative of the function (i.e., a “kink”). Indeed, a detailed analysis shows that there is a kink for  $y = y'$  (see Fig. 4); we can easily deal with it by writing

$$\frac{(k^2 + k'^2) k^2 k'}{(k^2 - k'^2) \Delta_{kk'}} = \frac{1}{8\pi^2 \varepsilon^2} \left( \frac{1}{k'(k^2 - k'^2)} - \frac{(k^2 - k'^2)}{k' \Delta_{kk'}} \right) \quad (66)$$

The summation can now be performed for the first term on the r.h.s of (66) and one obtains

$$\begin{aligned} \langle \delta\rho(y) \delta v(y') \rangle_{st} &= f(y, y') - \frac{4k_B \gamma}{\pi^3 S c \varepsilon} \\ &\times \sum_{k+k'=\text{odd}} \sum \cos\left(\frac{k\pi y}{L}\right) \sin\left(\frac{k'\pi y'}{L}\right) \frac{(k^2 - k'^2)}{k' \Delta_{kk'}} \end{aligned} \quad (67)$$

where

$$f(y, y') = \frac{k_B \gamma}{2TS} \left( \frac{1}{2} y' \left( 1 - \frac{y'}{L} \right) - \begin{cases} y'(1 - y/L) & \text{for } y' \leq y \\ y(1 - y'/L) & \text{for } y' \geq y \end{cases} \right) \quad (68)$$

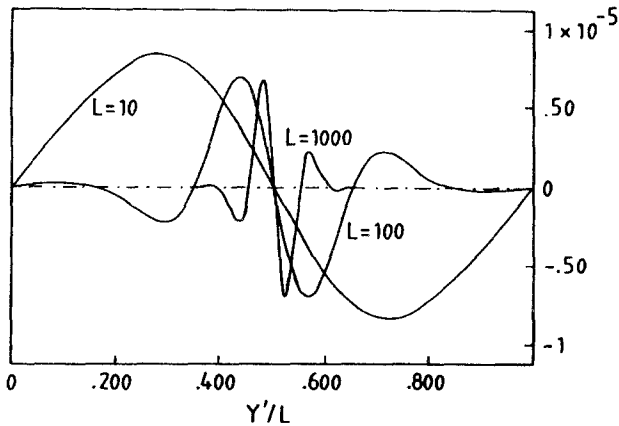


Fig. 3. The nonequilibrium component of  $\langle \delta v(y) \delta v(y') \rangle_{st}$  for  $y = L/2$  versus  $y'/L$ . The parameters are taken from the simulation described in Ref. 44 [ $T_0(y=0) = 1$ ,  $L_x = L_z = 1$ ,  $\eta_0 = 5/16\rho_0(\pi T_0)^{1/2}$ ,  $\zeta = 0$ ,  $c = (5/3k_B/mT_0)^{1/2}$ ,  $k_B/m = 1/2$ ,  $\rho_0 = 400$ ], with varying values of  $L$ . The system is under a constant temperature gradient,  $\gamma = 1/25$ .

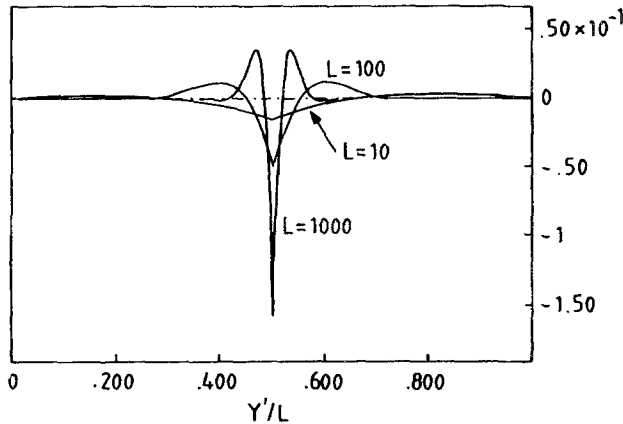


Fig. 4. The function  $\langle \delta\rho(y) \delta v(y') \rangle_{st}$  for  $y = L/2$  versus  $y'/L$ . The parameters are taken from the simulation described in Ref. 44 (see caption to Fig. 3) with varying values of  $L$ . The system is under a constant temperature gradient,  $\gamma = 1/25$ .

The double sum in (67) converges as  $O(k^{-5})$ , while the function  $f(y, y')$  contains the “kink.”

Let us now consider the asymptotic behavior of the static correlation functions in the limit  $\varepsilon \rightarrow 0$ . In contrast to the previous section, the sums cannot be transformed to intergals in a straightforward manner, since there are restrictions on the summation indices. For the sake of simplicity, we will restrict ourselves to the study of the correlations of the various quantities with respect to the center of the system. More precisely, we set system. More precisely, we set

$$y'/L = 1/2, \quad y/L = 1/2 + r, \quad -1/2 \leq r \leq 1/2 \tag{69}$$

Consider now, for example, the velocity autocorrelation function, as given by Eq. (62). Using (69), one finds

$$\begin{aligned} g_{vv}(r) &\equiv \left\langle \delta v \left( y = \frac{L}{2} + Lr \right) \delta v \left( y' = \frac{L}{2} \right) \right\rangle_{st} - \frac{k_B T_0(r)}{\rho_0 V} \delta(r) \\ &= \frac{16k_B \gamma}{\pi^2 \rho_0 S} \sum_{k \text{ even}} (-1)^{k/2} k \sin(k\pi r) \sum_{k' \text{ odd}} (-1)^{(k'-1)/2} \frac{k'}{\Delta_{kk'}} \end{aligned} \tag{70}$$

The sum over  $k'$  can now be easily performed by contour integration to yield

$$\begin{aligned} g_{vv}(r) &= \frac{k_B \gamma}{2\pi^2 \rho_0 S \varepsilon} \sum_{k \text{ even}} (-1)^{k/2} \frac{\sin k\pi r}{k^2 (\pi^2 \varepsilon^2 k^2 - 1)^{1/2}} \\ &\quad \times \left( \frac{1}{\cos \xi_+ \pi/2} - \frac{1}{\cos \xi_- \pi/2} \right) \end{aligned} \tag{71}$$

where

$$\xi_{\pm}^2 = \frac{1}{1 + 8\pi^2 \varepsilon^2 k^2} [1 - 4\pi^2 \varepsilon^2 \pm 4\pi \varepsilon k (\pi^2 \varepsilon^2 k^2 - 1)^{1/2}] \tag{72}$$

Expanding the various terms in powers of  $\varepsilon$ , one finds, to dominant order in  $\varepsilon$ ,

$$g_{vv}(r) \approx \frac{-4\pi k_B \gamma \varepsilon}{\rho_0 S} \sum_{k=1}^{\infty} k \sin(2k\pi r) \frac{\sinh(4\pi^2 k^2 \varepsilon)}{\cosh^2(4\pi^2 k^2 \varepsilon)} \tag{73}$$

Noticing that the summation index  $k$  can be rescaled by  $\sqrt{\varepsilon}$ , we can now take the limit  $\varepsilon \rightarrow 0$  to find

$$g_{vv}(r\varepsilon^{-1/2}) \equiv g_{vv}(R) \approx \frac{-4\pi k_B \gamma}{\rho_0 S} \int_0^{\infty} ds \sin(2\pi s R) \frac{\sinh(4\pi^2 s^2)}{\cosh^2(4\pi^2 s^2)} \tag{74}$$

An integration by parts leads to our final result,

$$g_{vv}(R) \approx \frac{-k_B \gamma}{2\pi \rho_0 S} R \int_0^{\infty} ds \frac{\cos(Rs)}{\cosh(s^2)}; \quad R = r\varepsilon^{-1/2} \tag{75}$$

Following the same line of calculation, we find for the static density autocorrelation function

$$\begin{aligned} g_{\rho\rho}(r) &\equiv \left\langle \delta\rho \left( y = \frac{L}{2} + Lr \right) \delta\rho \left( y' = \frac{L}{2} \right) \right\rangle_{\text{st}} - \frac{k_B T_0(y)}{\alpha V} \delta(r) \\ &\approx -\frac{k_B T_a}{\alpha V} - \frac{k_B \gamma}{2\pi \alpha S} R \int_0^{\infty} ds \frac{\cos(Rs)}{\cosh(s^2)} \end{aligned} \tag{76}$$

The first term in the rhs of (76) ensures the conservation of the total mass, while the second term is proportional to  $g_{vv}(R)$ .

Since  $|r| \leq 1/2$ ,  $R$  becomes infinity large in the limit  $\varepsilon \rightarrow 0$ , unless  $|r| \sim O(\sqrt{\varepsilon})$ . Using the series representation

$$\frac{1}{\cosh(s^2)} = 2\pi \sum_{k=1}^{\infty} \frac{(-1)^{k+1} (k-1/2)}{s^4 + \pi^2 (k-1/2)^2} \tag{77}$$

it is easy to check that, in the limit  $R \rightarrow \infty$ , we have

$$\begin{aligned} g_{vv}(R) &\sim \frac{-k_B \gamma}{2\sqrt{\pi} \rho_0 S} R \exp\left(\frac{-R\sqrt{\pi}}{2}\right) \sin\left(\frac{R\sqrt{\pi}}{2} + \frac{\pi}{4}\right) \\ &\quad + O\left(\exp\frac{-R\sqrt{3\pi}}{2}\right) \end{aligned} \tag{78}$$

In other words, for any given value of  $r$ , the nonequilibrium contribution to the static velocity and density autocorrelation function behaves as  $O[\exp(-1/\sqrt{\varepsilon})]$  and therefore vanishes exponentially with the system size. On the other hand, for fixed  $L$ , the above correlation functions are significantly different from zero only for  $|r| \sim O(\sqrt{\varepsilon})$ . Their correlation lengths are therefore of the order of the square root of the system size  $\sqrt{L}$ .

These asymptotic results are nicely supported by the numerical evaluations of the corresponding series [see Eq. (62) and Fig. 3]. Although the correlation length is large, the entire function vanishes in the limit of infinite systems. This is an important result, since it proves that in the presence of a temperature gradient, the existence of the above oscillatory, long-ranged correlation functions are entirely due to the boundary effects.

This, however, is not the case for the density-velocity (or density-current) static correlation function. In fact, proceeding as before, one finds, to dominant order in  $\varepsilon$ ,

$$g_{\rho v}(r) \equiv \left\langle \delta\rho\left(y = \frac{L}{2} + Lr\right) \delta v\left(y' = \frac{L}{2}\right) \right\rangle \\ \approx -\frac{k_B\gamma}{2\pi cS} \frac{1}{\sqrt{\varepsilon}} \int_0^\infty ds \frac{\cos(Rs)}{s^2} \left(1 - \frac{1}{\cosh(s^2)}\right) \quad (79)$$

The exact asymptotic analysis of the integral in (79) is quite complicated and we were not able to express the result in a closed form. Nevertheless, a qualitative analysis can be made using the following arguments: the kernel  $s^{-2}[1 - 1/\cosh(s^2)]$  behaves as  $(1 + s^2/12)/2$  in the limit  $s \rightarrow 0$  and as  $1/s^2$  in the limit  $s \rightarrow \infty$ . Therefore, for any fixed value of  $r \neq 0$ , the integral in (79) is *qualitatively* comparable to

$$12 \int_0^\infty ds \cos(Rs) \frac{1 + s^2}{24 + s^4}$$

which behaves essentially as  $g_{vv}(R)$ , Eq. (78). So again, the function  $g_{\rho v}(R)$  is significantly different from zero for  $|r| \sim O(\sqrt{\varepsilon})$ . But now, because of the presence of the  $1/\sqrt{\varepsilon}$  factor in front of the integral,  $g_{\rho v}(r)$  grows as  $\sqrt{L}$  in the limit  $L \rightarrow \infty$ . For instance, in the case  $r = 0$ , one easily finds

$$g_{\rho v}(0) \approx -\frac{k_B\gamma}{\pi S c} \frac{1}{\sqrt{\varepsilon}} \int_0^\infty ds \frac{\sinh(s^2)}{\cosh^2(s^2)} \approx -0.49 \frac{k_B\gamma}{\pi S} \left(\frac{L}{c\Gamma}\right)^{1/2} \quad (80)$$

The nonequilibrium contribution to the density-velocity correlation function has therefore an intrinsic origin, independent of the boundaries. In small systems, such as those realized in computer experiments, the boun-

dary effects can be as important as the intrinsic effect and therefore the full problem must be considered.

The behavior of the above static correlation functions clearly suggests the existence of stationary sound waves generated by density fluctuations. To check this hypothesis, we have to compute the dynamical correlation functions as well. The explicit time-dependent problem, in the presence of a temperature gradient, proves however to be quite difficult to handle. Nevertheless, the scattering function can still be computed exactly<sup>(48)</sup> and in the next section we examine its equilibrium and nonequilibrium properties in finite systems.

### 5. SCATTERING FUNCTION

In this section we consider in detail the dynamic correlation function for density fluctuations. Concentrating on the scattering function, as defined by Eq. (19), we obtain its explicit form, including nonequilibrium and finite-size effects. This scattering function is equivalent, in the hydrodynamic limit, to the Van Hove total correlation function [Eq. (18)]. Though most of the analysis is general, our aim is to obtain the scattering function for the range of parameters appropriate to computer experiments.

Consider the density autocorrelation function in  $(k, \omega)$  space as given by Eq. (56). Taking the inverse Fourier transform and using the definition of  $T_{kk'}$  [Eq. (59)], one finds

$$\begin{aligned} &\langle \delta\rho(y, \omega) \delta\rho(y', \omega') \rangle \\ &= \frac{4k_B \Gamma \rho_0}{\pi V(c^4 + 4\omega^2 \Gamma^2)} \frac{2}{L} \int_0^L d\xi T_0(\xi) \Xi(y, \xi) \Xi^*(y', \xi) \end{aligned} \quad (81)$$

with

$$\begin{aligned} \Xi(y, \xi) &= \sum_{k=0}^{\infty} \cos\left(\frac{k\pi y}{L}\right) \cos\left(\frac{k\pi \xi}{L}\right) \frac{k^2}{k^2 - z^2} \\ &= \frac{L}{2} \delta(y - \xi) - \frac{\pi}{4} \frac{z}{\sin \pi z} \left\{ \cos \left[ \pi z \left( 1 - \frac{|y - \xi|}{L} \right) \right] \right. \\ &\quad \left. + \cos \left[ \pi z \left( 1 - \frac{y + \xi}{L} \right) \right] \right\} \end{aligned} \quad (82)$$

where  $z$  is defined by Eq. (60). From (81), the scattering function can now easily be computed, and after some tedious algebra, one finds

$$\begin{aligned}
 S_q(\omega) = & \frac{32k_B T_a}{\pi m c^4} \frac{\Gamma q^2}{(\omega^2 L^2 / \pi^2 c^2 - 4q^2)^2 + 64q^4 \omega^2 \Gamma^2 / c^4} \\
 & \times \operatorname{Re} \left[ q^2 + \frac{4q^2}{\pi(4q^2 - z^2)} z \tan \frac{\pi z}{2} \right. \\
 & + \frac{|z|^2}{4\pi |\cos(\pi z/2)|^2} \left( \frac{\sin[\pi(z - z^*)/2]}{z - z^*} - \frac{\sin[\pi(z + z^*)/2]}{z + z^*} \right) \\
 & \left. + \frac{\gamma L}{T_a} q \frac{iz^2}{\pi(4q^2 - z^2)} \left( 1 + \frac{2(z^2 + 4q^2)}{\pi z(4q^2 - z^2)} \tan \frac{\pi z}{2} \right) \right] \quad (83)
 \end{aligned}$$

where  $T_a$  is the (space) averaged temperature. We plot the exact solution (83) in Fig. 5 for thermodynamic equilibrium (i.e.,  $\gamma=0$ ) and in Fig. 6 a nonequilibrium case (in each case  $q=1$ ). Besides the usual Brillouin lines<sup>(53)</sup> (located at  $\omega \approx \pm 0.15$ ), one also sees two sharp peaks at lower frequency. For this model, we have no Rayleigh line (central peak), because setting the thermal expansion coefficient to zero implies that the specific heats at constant pressure and volume are equal.

Let us now consider our exact expression (83) in the limit of small  $q$  (e.g., 1 or 2) and assume that  $L$  is large enough so that we may restrict our

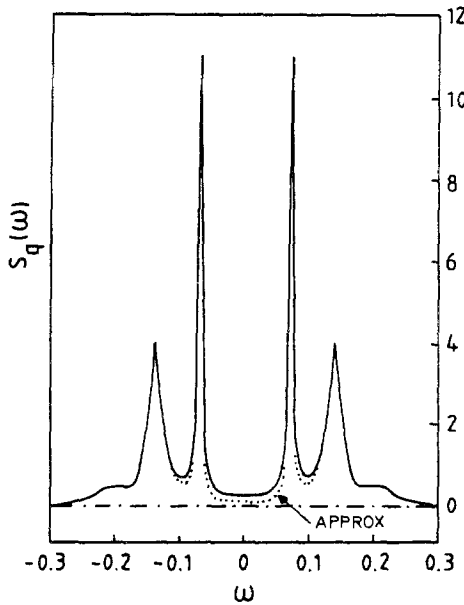


Fig. 5. The scattering function  $S_q(\omega)$  as a function of frequency for  $q=1$  and  $\gamma=0$  (equilibrium). The parameters are taken from the simulation described in Ref. 44 (see caption to Fig. 3), with the exception that we take  $\Gamma=7\eta_0/(6\rho_0)$ .

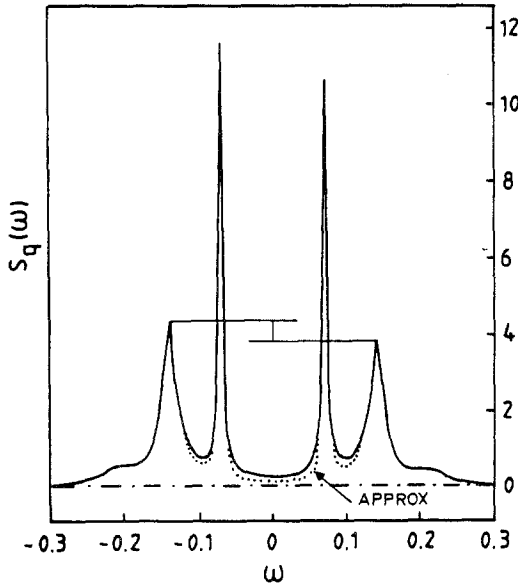


Fig. 6. The scattering function  $S_q(\omega)$  as a function of frequency for  $q=1$  and temperature gradient  $\gamma = 1/25$ . See caption to Fig. 5 for more details.

analysis to values of  $\omega$  of the order of  $c/L$ . Note that this is not the appropriate regime for the study of macroscopic systems, such as those studied in light scattering experiments.<sup>(48)</sup> In computer experiments, however, the wavelength ( $L/q$ ) on which the dynamic correlations are measured will have to be of the order of the system size if one wishes to remain in the hydrodynamic regime. Moreover, in a dilute gas simulation, the statistical error in the data constrains one to consider only the zero wavenumber in the parallel direction (i.e., reduced variables). The limit we are considering is thus appropriate for comparison with particle simulations. With this understanding, after some algebra one finds

$$\begin{aligned}
 S_q(\omega) \approx & \frac{k_B \rho_0 T_a \chi_T}{\pi m} \left[ \frac{16q^4 \Gamma / c^2}{(\omega^2 L^2 / \pi^2 c^2 - 4q^2)^2 + 64q^4 \omega^2 \Gamma^2 / c^4} \right. \\
 & \times \left( 1 - \frac{32 \gamma q^5 \pi^3}{3 T_a L} \frac{\omega \Gamma^3 / c^4 (\omega^2 L^2 / \pi^2 c^2 + 4q^2)}{(\omega^2 L^2 / \pi^2 c^2 - 4q^2)^2 + 64q^4 \omega^2 \Gamma^2 / c^4} \right) \\
 & + \left( \frac{4q}{c\pi(\Theta_k^2 - 4q^2)} \right)^2 \frac{L^2 \omega^2 \Gamma}{2c^2(1 + \cos L\omega/c) + L^2 \omega^4 \Gamma^2 / c^4} \\
 & \left. \times \left( 1 - \frac{8\gamma q \omega \Gamma L}{\pi c^2 T_a} \frac{\Theta_k^2 + 4q^2}{(\Theta_k^2 - 4q^2)^2} \right) \right] \quad (84)
 \end{aligned}$$

where

$$\Theta_k = 2k - 1 \quad \text{for} \quad 4(k-1)^2 \leq L^2 \omega^2 / \pi^2 c^2 < 4k^2; \quad k = 1, 2, \dots \quad (85)$$

and

$$\chi_T = (\partial \rho_0 / \partial P_0)_{T_0} / \rho_0 \equiv 1 / (\alpha \rho_0^2)$$

is the isothermal compressibility. The first term yields the Brillouin lines; its maxima are at  $\omega L/c = \pm 2\pi q$ . The second term reflects the finite-size effect and is responsible for the extra peaks, which occur for  $\omega L/c = \pm \pi, \pm 3\pi, \dots$ . Each of these terms is composed of two parts, an equilibrium part and a nonequilibrium part which is proportional to the temperature gradient  $\gamma$ . The absence of terms nonlinear in the gradient is a result of our first two assumptions (see Section 2). In Figs. 5 and 6, we see that the approximation is already quite good, at least near the peaks, for the parameters of the computer simulation described in Ref. 44 ( $L/c \approx 50$  mean free times). The comparison with recent computer simulation data also shows nice qualitative agreement with these results. Specifically, the extra peaks are observed and they are found to be asymmetric out of equilibrium.<sup>(57)</sup>

The nonequilibrium terms are seen to be odd in frequency, yielding the asymmetry seen in Fig. 6. The part corresponding to the Brillouin lines is a double Lorentzian, in agreement with previous calculations where the boundary effects are neglected.<sup>(45)</sup> Its coefficient, however, is different as a direct result of the dominant role of the boundaries. To see this, let us consider in more detail the origin of the asymmetry in the spectrum. Satten and Ronis<sup>(48)</sup> found a modulation of the Brillouin lines because of the boundary effect and a smaller asymmetry than that obtained in calculations where the boundary effects were neglected. In our case, the finite-size peaks do not overlap with the Brillouin lines, but are well separated. Yet a detailed analysis of the various terms in the exact expression (83) shows that the asymmetry arises mainly from the finite-size effect (see Ref. 58 for the full discussion of this result). It is clear that for macroscopic systems, such as laboratory systems used in light scattering experiments, the interplay between bulk and boundary effects will be different. Though nonlinear effects are not considered in our analysis,<sup>(20,59)</sup> for computer experiments, due to the small system size and the presence of stochastic boundaries, the finite-size effect seems to dominate over nonlinear effects even though the imposed nonequilibrium constraints are extremely large. Note that in a recent work dealing with macroscopic systems, Schmitz and Cohen arrive essentially at the same conclusion.<sup>(60)</sup>

Consider now the finite-size peaks; an obvious explanation for the

extra lines at odd values of  $\omega L/\pi c$  is the existence of stationary sound waves across the system, as originally suggested in Refs. 61 and 62 for equilibrium systems and later remarked in Ref. 48 for nonequilibrium systems. The density fluctuations are converted to sound waves, which are reflected by the rigid walls, giving rise to stationary waves. For this picture to be consistent, however, we have to check two consequences. First, for a system with periodic boundary conditions in the  $y$  directions, the extra peaks must disappear, since for the stationary waves to be formed, one needs coherent sound waves crossing. It is easy to check theoretically that this is indeed so. It is also known from equilibrium computer simulation measurements that there are no such peaks (some other effects can, however, be observed if the time correlation functions are considered for lag times greater than the sound crossing time in the system<sup>(34,63)</sup>).

Next, the perpendicular-current static correlation function must obviously contain this effect. At equilibrium this function is delta-correlated. The random distribution of the phases of the Langevin sources ensures time-reversal symmetry and thus eliminates any observable effect in this function. In nonequilibrium systems, however, the average amplitudes of the Langevin sources are not equal and the standing waves produce an observable effect. Recall the (perpendicular) velocity-velocity static correlation function, given by Eq. (62) and represented in Fig. 3. Its form clearly suggests the existence of spatially damped standing waves across the system. As demonstrated in the previous section, in the limit of large  $L$ , the nonequilibrium contribution to  $\langle \delta v(y) \delta v(y') \rangle_{st}$  and  $\langle \delta \rho(y) \delta \rho(y') \rangle_{st}$  goes to zero as  $L \rightarrow \infty$ . This, however, was not the case for the density-current static correlation function, since it arises from the broken time-reversal symmetry and is responsible for the asymmetry in the Brillouin lines, even in an infinite medium.<sup>(45)</sup> These properties of the static correlation function and the presence of extra peaks in  $S_q(\omega)$  definitely establish the presence of standing waves across the system generated by fluctuations. They also show the existence of long-range oscillatory correlation functions and the dominant role of the boundary effects on the statistical properties of nonequilibrium systems. From an experimental point of view, the effect is difficult to observe in light scattering measurements, as discussed in Ref. 48.

At the end of Section 3 we mentioned that there is no nonequilibrium effect on the reduced density fluctuations in a system under shear. Thus, the equilibrium scattering function obtained in this section applies equally well to a system with a velocity gradient but without a temperature gradient (negligible viscous heating). Again we point out that there is no shear-induced modification to the scattering function, because our use of reduced variables (cf. Section 3).

## 6. CONCLUSION

In this paper we have studied the statistical properties of a simple fluid in finite systems and under nonequilibrium constraints. Our main goal was to obtain exact expressions for the static and dynamic correlation functions so that the results could be compared with those obtained in computer experiments. The mathematical analysis of the problem proves to be rather involved, mainly because of the boundary value problem. In this paper we have emphasized finite-size effects at the expense of studying a somewhat simplified scenario. We had to restrict ourselves to a model fluid for which the thermal expansion coefficient is zero and the transport coefficients are constant. A further simplification is introduced by limiting our analysis to the study of reduced variables, i.e., setting the “parallel” Fourier components to zero. When the exact expressions for the various correlation functions did not possess a clear compact form, we explored their asymptotic behavior, in the limit of a large system size, to extract the relevant physics.

The fluid is assumed to be confined between two parallel plates acting as infinite reservoirs so that, by fixing their temperatures and velocities, one can impose the desired nonequilibrium constraints on the system. The boundary conditions are those realized in typical molecular dynamics simulations: fixed temperature and velocities at the walls and periodic boundary conditions in the other directions (parallel to the walls). Two scenarios were envisaged: a system under a constant shear and a system under a constant temperature difference.

The first conclusion is that many of the correlation functions are *not* affected by either the boundaries or the nonequilibrium constraints. For example, when a velocity gradient is imposed,  $\langle \delta\rho(y) \delta\rho(y') \rangle_{st}$ ,  $\langle \delta\rho(y) \delta v(y') \rangle_{st}$ , and  $\langle \delta v(y) \delta v(y') \rangle_{st}$  are unaffected by the shear, while  $\langle \delta u(y, t) \delta u(y', t') \rangle$  and  $\langle \delta w(y, t) \delta w(y', t') \rangle$  retain their equilibrium form in spite of the presence of a temperature gradient. In some cases, the absence of an effect is a direct consequence of the simplicity of our model fluid or the use of reduced variables. Yet it is interesting to note that, while the correlation functions for some reduced variables change dramatically out of equilibrium, others remain entirely unaffected.

Second, the static correlation functions that are affected by the nonequilibrium constraints are all long-ranged. Some correlations [e.g.,  $\langle \delta u(y) \delta u(y') \rangle_{st}$  for shear and  $\langle \delta\rho(y) \delta v(y') \rangle_{st}$  for temperature gradient] extend over the entire system and persist even in the limit of large system size  $L$  (see Figs. 1 and 4). They therefore have an intrinsic origin in the sense that the finite-size effects give rise only to a quantitative correction, which becomes vanishingly small as the system size becomes large. Others,

such as  $\langle \delta v(y) \delta v(y') \rangle_{st}$  and  $\langle \delta \rho(y) \delta \rho(y') \rangle_{st}$  in a system with a temperature gradient, have a characteristic range of the order of  $\sqrt{L}$ , but their amplitude, although proportional to the temperature gradient, eventually vanishes in the limit  $L \rightarrow \infty$  (gradient fixed). They therefore have an extrinsic origin in the sense that the nonequilibrium modifications exist only because of the boundary effects; in the limit of infinitely large systems, these correlation functions take their equilibrium form. Our asymptotic analysis shows that the dimensionless quantity

$$\varepsilon = \frac{\text{kinematic viscosity}}{\text{sound speed} \cdot \text{system length}}$$

plays an important role in delineating the characteristic regimes (Section 4). As we have shown, to dominant order in  $\varepsilon$ , the various correlation functions are naturally scaled by  $\varepsilon^{-1/2}$ , i.e.,

$$\langle \delta a(y) \delta b(y') \rangle_{st} = f[\varepsilon^{-1/2}(y - y')/L] \quad (86)$$

where  $a$  and  $b$  represent the density or the velocity fluctuations. This the parameter that controls the effective correlation lengths of fluctuating variables. Its inverse,  $\varepsilon^{-1}$ , resembles the Reynolds number except that the characteristic velocity is now replaced by the sound velocity. Note, finally, that the long-range coherence of fluctuations emphasizes the necessity of carefully dealing with the boundary conditions even for large systems.

Third, given the interesting modifications observed in the static correlation functions, it is not surprising to find these effects reflected in the dynamic correlation functions. It is well known that the Brillouin lines in the scattering function become asymmetric when the fluid is subjected to a temperature gradient.<sup>(45)</sup> In equilibrium systems, because of time-reversal symmetry, the static density-current correlation function is zero. In the presence of a temperature gradient, however, the time-reversal symmetry is broken;  $\langle \delta \rho(y) \delta v(y') \rangle_{st}$  is no longer zero (Section 4) and, as a consequence, the Brillouin lines are asymmetric. In Section 5, we demonstrated a finite-size effect in the scattering function, the appearance of extra peaks in the spectrum. These extra peaks indicate the existence of standing sound waves generated by the fluctuations. Interestingly, they are *also* asymmetric out of equilibrium in the same manner as the Brillouin lines. We believe this effect to be a reflection of the nonequilibrium modifications of the static correlation functions  $\langle \delta \rho(y) \delta \rho(y') \rangle_{st}$  and  $\langle \delta v(y) \delta v(y') \rangle_{st}$ .

As we already emphasized, our main goal in this article was to compare our results with those obtained from particle simulations. Molecular dynamics methods are too slow and thus far have only yielded qualitative results.<sup>(40,41)</sup> Computational model fluids, such as cellular automata, have

proven to be useful in describing macroscopic hydrodynamic flows, mainly due to their high computational speed.<sup>(64)</sup> Unfortunately, the problem of defining a thermodynamic temperature precluded the study of hydrodynamic fluctuations (see, however, Ref. 65).

Recently, we have employed stochastic particle simulations<sup>(42)</sup> (based on the Boltzmann equation) to measure nonequilibrium correlation functions in a dilute gas.<sup>(43,44,56)</sup> It is surprising to note that in spite of the strong assumptions made in our fluid model, as compared with dilute gas hydrodynamics, all of our results agree, at least qualitatively, with the available data. This is true for both the shear and temperature gradient cases. Very recently, the finite-size peaks have also been observed in such simulations<sup>(57)</sup>; the results are again in qualitative agreement with our analysis.

Finally, it should be pointed out that our model fluid suffers from two handicaps. First, setting the thermal expansion coefficient to zero precludes a study of the Rayleigh line. Second, we have only treated the reduced variables throughout this paper. While these limitations are perhaps regrettable, our results mark a necessary step toward the more complete theory that we are currently developing.

## APPENDIX: MATHEMATICAL PROPERTIES OF THE SOLUTIONS

In this Appendix, we demonstrate that the initial conditions  $\{\delta\rho(y, t=0), \delta\mathbf{u}(y, t=0)\}$  and the boundary conditions for  $\delta\mathbf{u}$

$$\delta\mathbf{u}(y=0, t) = \delta\mathbf{u}(y=L, t) = 0 \quad (\text{A1})$$

are sufficient to specify the solution of Eqs. (8)–(11). In particular, we show that a boundary condition for the density cannot be specified. To do so, it is sufficient to consider the homogeneous (i.e., no source terms) equations for  $\delta\rho$  and  $\delta v$ ,

$$\partial\delta\rho/\partial t = -\rho_0 \partial\delta v/\partial y \quad (\text{A2})$$

$$\partial\delta v/\partial t = -\alpha \partial\delta\rho/\partial y + \eta/\rho_0 \partial^2\delta v/\partial y^2 \quad (\text{A3})$$

The solutions for  $\delta u$  and  $\delta w$  follow directly given  $\delta v$ , since the former are not coupled to  $\delta\rho$ .

What we have to prove is that the uniqueness of the solution does not require the specification of a boundary condition for  $\delta\rho$ , i.e., the system itself determines the particular value of  $\delta\rho$  at the boundaries. To this end, let us consider the auxiliary function

$$A(t) \equiv \int_0^L dy [\alpha(\delta\rho)^2 + \rho_0(\delta v)^2] \geq 0 \quad (\text{A4})$$

This function may be associated with the total acoustic energy in the system. It follows from direct calculation that if  $\{\delta\rho(y, t), \delta\mathbf{u}(y, t)\}$  is a solution of (A2)–(A3) that satisfies the boundary condition (A1), then  $\partial A/\partial t \leq 0$  (recall that  $\alpha$ ,  $\rho_0$ , and  $\eta$  are positive).

Consider now the quiescent initial condition  $\{\delta\rho(y, t=0)=0, \delta\mathbf{u}(y, t=0)=0\}$ . Clearly,  $A(t=0)=0$ , so, from our result,  $A(t)=0$  for all  $t$ . From the definition (A4), this implies that the only solution is  $\{\delta\rho(y, t)=0, \delta\mathbf{u}(y, t)=0\}$  for all  $t$ . Our proof of uniqueness is now standard. Assume that there exist two solutions  $\{\delta\rho_1, \delta\mathbf{u}_1\}$  and  $\{\delta\rho_2, \delta\mathbf{u}_2\}$ , which satisfy the same arbitrary initial condition and the boundary condition (A1). The difference  $\{\delta\rho_1 - \delta\rho_2 = \delta\tilde{\rho}, \delta\mathbf{u}_1 - \delta\mathbf{u}_2 = \delta\tilde{\mathbf{u}}\}$  must also be a solution satisfying the boundary condition and the initial condition  $\{\delta\tilde{\rho}(y, t=0)=0, \delta\tilde{\mathbf{u}}(y, t=0)=0\}$ . From our previous result,  $\{\delta\rho_1 - \delta\rho_2 = 0, \delta\mathbf{u}_1 - \delta\mathbf{u}_2 = 0\}$ , completing the proof of uniqueness.

## ACKNOWLEDGMENTS

We wish to thank Prof. G. Nicolis, Dr. M. Mareshal, Dr. G. Lie, and Dr. D. Kondepudi for stimulating discussions and helpful comments. We wish to thank Prof. I. Prigogine for his encouragement and insightful suggestions.

## REFERENCES

1. G. Nicolis and I. Prigogine, *Self-Organisation in Nonequilibrium Systems* (Wiley, New York, 1977).
2. H. Haken, *Z. Physik B* **20**:413 (1975).
3. C. W. Gardiner, K. J. McNeil, D. F. Walls, and I. S. Matheson, *J. Stat. Phys.* **14**:307 (1976).
4. H. Lemarchand and G. Nicolis, *Physica* **82A**:251 (1976).
5. G. Nicolis and M. Malek Mansour, *Phys. Rev. A* **29**:2845 (1984).
6. G. Nicolis and M. Malek Mansour, *J. Stat. Phys.* **22**:495 (1980).
7. M. Malek Mansour, C. Van den Broeck, G. Nicolis, and J. W. Turner, *Ann. Phys. (N.Y.)* **131**:283 (1981).
8. H. Lemarchand, *Physica* **101A**:518 (1980); H. Lemarchand and G. Nicolis, *J. Stat. Phys.* **37**:609 (1984).
9. D. Walgraef, G. Dewel, and P. Borckmans, *Phys. Rev. A* **21**:397 (1980).
10. D. Walgraef, G. Dewel, and P. Borckmans, *Adv. Chem. Phys.* **49**:311 (1982).
11. L. D. Landau and E. M. Lifschitz, *Fluid Mechanics* (Pergamon Press, Oxford, 1959).
12. I. Procaccia, D. Ronis, and I. Oppenheim, *Phys. Rev. Lett.* **42**:287 (1979).
13. D. Ronis, I. Procaccia, and I. Oppenheim, *Phys. Rev. A* **19**:1324 (1979).
14. T. R. Kirkpatrick, E. G. D. Cohen, and J. R. Dorfman, *Phys. Rev. Lett.* **42**:862 (1979).
15. T. R. Kirkpatrick, E. G. D. Cohen, and J. R. Dorfman, *Phys. Rev. Lett.* **44**:472 (1980).
16. D. Beysens, Y. Garrabos, and G. Zalczler, *Phys. Rev. Lett.* **45**:403 (1980).
17. D. Beysens, *Physica* **118A**:250 (1983).
18. R. Penney, H. Kieft, and J. M. Clouter, *Bull. Can. Assoc. Phys.* **39**:BB8 (1983).
19. G. H. Wegdam, N. M. Keulen, and J. C. F. Michiels, *Phys. Rev. Lett.* **55**:630 (1985).

20. T. R. Kirkpatrick and E. G. D. Cohen, *Phys. Lett.* **78A**:350 (1980).
21. T. R. Kirkpatrick, E. G. D. Cohen, and J. R. Dorfman, *Phys. Rev. A* **26**:950 (1982).
22. D. Ronis and I. Procaccia, *Phys. Rev. A* **26**:1812 (1982).
23. D. Ronis and S. Putterman, *Phys. Rev. A* **22**:773 (1980).
24. A. M. Tremblay, M. Arai, and E. D. Siggia, *Phys. Rev. A* **23**:1451 (1981).
25. G. Van der Zwan, D. Bedaux, and P. Mazur, *Physica* **107A**:491 (1981).
26. J. W. Dufty, in *Spectral Line Shapes*, P. Wende ed. (de Gruyter, Berlin, 1981).
27. J. Machta, I. Procaccia, and I. Oppenheim, *Phys. Rev. Lett.* **42**:1368 (1979).
28. J. Machta, I. Oppenheim, and I. Procaccia, *Phys. Rev. A* **22**:2809 (1980).
29. B. Alder, D. Gass, and T. Wainwright, *J. Chem. Phys.* **53**:3813 (1976).
30. B. Alder and T. Wainwright, *Phys. Rev. A* **1**:18 (1970).
31. D. J. Evans, *Phys. Lett.* **74A**:229 (1979).
32. D. J. Evans and G. P. Morriss, *Phys. Rev. Lett.* **51**:1776 (1983).
33. J. J. Erpenbeck, *Phys. Rev. Lett.* **52**:1333 (1984).
34. J. P. Boon and S. Yip, *Molecular Hydrodynamics* (McGraw-Hill, New York, 1980).
35. E. Meiburg, *Phys. Fluids* **29**:3107 (1986); L. Hannon, G. Lie and E. Clementi, *J. Sc. Comp.* **1**:145 (1986).
36. D. Rappaport and E. Clementi, *Phys. Rev. Lett.* **57**:695 (1987).
37. M. Mareschal and E. Kestemont, *J. Stat. Phys.* **48**:1187 (1987).
38. D. J. Evans and W. G. Hoover, *Annu. Rev. Fluid Mech.* **18**:243 (1986).
39. G. Ciccoti and A. Tenenbaum, *J. Stat. Phys.* **23**:767 (1981); A. Tenenbaum, G. Ciccoti, and R. Gallio, *Phys. Rev. A* **25**:2778 (1982); A. Tenenbaum, *Phys. Rev. A* **28**:3132 (1983).
40. M. Mareschal and E. Kestemont, *Phys. Rev. A* **30**:1158 (1984).
41. L. Hannon, private communication.
42. G. A. Bird, *Molecular Gas Dynamics* (Clarendon Press, Oxford, 1976).
43. A. Garcia, *Phys. Rev. A* **34**:1454 (1986).
44. M. Malek Mansour, A. Garcia, G. Lie, and E. Clementi, *Phys. Rev. Lett.* **58**:874 (1987).
45. A. M. Tremblay, in *Recent Developments in Nonequilibrium Thermodynamics*, J. Casas-Vasquez, D. Jou, and G. Lebon, eds. (Springer-Verlag, Berlin, 1984).
46. R. P. Behringer, *Rev. Mod. Phys.* **57**:657 (1985).
47. A. M. Tremblay, E. D. Siggia, and M. R. Arai, *Phys. Lett.* **76A**:57 (1980).
48. G. Satten and D. Ronis, *Phys. Rev. A* **26**:940 (1982).
49. A. Garcia, M. Malek Mansour, G. Lie, and E. Clementi, *J. Stat. Phys.* **47**:209 (1987).
50. L. D. Landau and E. M. Lifschitz, *Statistical Physics* (Pergamon Press, Oxford, 1959).
51. J. L. Lebowitz and H. Spohn, *J. Stat. Phys.* **19**:633 (1978).
52. P. Résibois and M. DeLeener, *Classical Kinetic Theory of Fluids* (Wiley, New York, 1977).
53. B. J. Berne and R. Pecora, *Dynamic Light Scattering* (Wiley, New York, 1976).
54. A. Garcia, *Phys. Lett.* **119**:379 (1987).
55. H. Spohn, *J. Phys. A* **16**:4275 (1983).
56. A. Garcia, M. Malek Mansour, M. Mareschal, G. Lie, and E. Clementi, *Phys. Rev. A* (in press).
57. G. Lie, preprint.
58. M. Malek Mansour, A. Garcia, J. W. Turner, and M. Mareschal, *Phys. Rev. A* (1987), submitted.
59. T. R. Kirkpatrick, E. G. D. Cohen, and J. R. Dorfman, *Phys. Rev. A* **26**:995 (1982).
60. R. Schmitz and E. G. D. Cohen, *Phys. Rev. A* **35**:2602 (1987).
61. D. Gutkowisc-Krusin and I. Procaccia, *Phys. Rev. Lett.* **48**:417 (1982).
62. D. Gutkowisc-Krusin and I. Procaccia, *Phys. Rev. A* **27**:2585 (1983).
63. W. E. Alley, B. J. Alder, and S. Yip, *Phys. Rev. A* **27**:3174 (1983).
64. S. Wolfram, *J. Stat. Phys.* **45**:471 (1986).
65. N. Margolus, T. Toffoli, and G. Vichniac, *Phys. Rev. Lett.* **56**:1695 (1986).